International Journal of Bioelectromagnetism
Vol. 9, No. 4, pp. 270 - 275, 2007
www.ijbem.org

Correlation between Independent Components of scalp EEG and intra-cranial EEG (iEEG) time series

Elsa van der Loo[a], Marco Congedo[b], Mark Plazier[a], Paul Van de Heyning[a], Dirk De Ridder[a]

[a]*Brain Research centre Antwerp for Innovative and Interdisciplinary Neuromodulation (BRAI²N), Edegem,Belgium*

[b]*National Center for Scientific Research (CNRS), GIPSA-lab, Grenoble, France*

Correspondence: E. van der Loo, University Hospital Antwerp, Wilrijkstraat 10, 2560 Edegem, Belgium. E-mail: elsa.vanderloo@ua.ac.be , phone +323 821 56 08

Abstract. 19 scalp electrode (EEG) and 8 intra-cranial electrode (iEEG) are recorded simultaneously with a common reference. EEG data is subjected to independent component analysis (ICA) and localisation of components in grey matter is estimated by the sLORETA inverse solution. Correlation between the time series of two independent components and intra-cranial recordings is very high (computed over 23552 samples, max r = 0.8 and 0.67, respectively). One component is localized underneath the site of the implanted electrode. These findings were replicated using the second row of 8 iEEGs and an independent 19-electrode EEG recording, validating the source localisation provided by combining ICA and sLORETA.

Keywords: Intra-cranial recording; Independent Component Analysis; ICoN; Tinnitus; sLORETA

1. Introduction

Since the increasing interest in localizing brain activity and understanding various pathological and physiological states, various techniques have been used to trace brain activity. EEG offers a non-invasive way to measure spontaneous brain activity with a high temporal resolution, but low spatial resolution. Source estimation methods solving the inverse-problem have been developed enabling approximate localization of brain activity in a 3D brain-space. In this study we couple the standardized Low-Resolution Electromagnetic Tomography (sLORETA) (Pascual-Marqui, 2002) with Independent Component Analysis (ICA) (Cichocki and Amari, 2002). ICA in this context may be conceived as a spatial filter enhancing the resolution and reliability of sLORETA estimations.

Recently extra-dural auditory cortex electrode implantations were proposed as a therapy for tinnitus (De Ridder et al., 2007). Cortical electrical stimulation completely or partially relieves patients from their phantom sound, when it is delivered to auditory areas. The presence of these intracranial electrodes offers the possibility to compare scalp EEG activity with simultaneously recorded intra-cranial electrode activity. This gives us the opportunity to validate the source components calculated from the EEG by correlating the time-series of these simultaneously recorded scalp and intra-cranial activities.

2. Material and Methods

Auditory cortex implantation was performed through a neuronavigated fMRI-guided placement of a 16 polar electrode (Lamitrode 88, ANS Medical, Plano, TX, USA) on the dura overlying the area of BOLD signal change associated with the tinnitus pitch on the auditory cortex. Patient KV (27 years, female), suffering from right unilateral white noise tinnitus, underwent this procedure on the left contra-lateral auditory cortex (see Fig. 1) at the multidisciplinary tinnitus clinic of the University Hospital of Antwerp, Belgium. The local ethical committee approved all aspects of the study.

Scalp and intra-cranial EEG (iEEG) recordings were performed simultaneously in relaxed state over 5 minutes with eyes opened in a sound proof and electromagnetically shielded room using

Synamps2 equipment (Neuroscan Inc.). For EEG, nineteen electrodes (Fp1, Fp2, F7, F3, Fz, F4, F8, T3, C3, Cz, C4, T4, T5, P3, Pz, P4, T6, O1, O2) were used following the 10-20 system. iEEG was simultaneously recorded on poles 1-8 (lower row, anterior to posterior) and 9-16 (upper row, anterior to posterior) of the intra-cranial electrode separately (see Fig. 1). For both EEG and iEEG the sampling rate was 1000Hz (band-pass: 0.15-200Hz), the impedance was checked to remain below 6 kΩ and the reference was a scalp electrode near the vertex. For the sake of validity of the ensuing multivariate analysis, we stress the importance to have both EEG and iEEG sharing the same reference.

Scalp EEG and poles 1-8 of the iEEG were band-pass filtered between 1-44Hz and down-sampled to 128Hz. After removal of instrumental artifacts, 184 seconds were left for analysis. EEG was referenced to the common average. Because of the common average reference one dimension is lost in the sensor space (Congedo, 2006), thus the space of EEG data is first reduced to 18 by principal component analysis. EEG ICA was performed using approximate joint diagonalization of Fourier co-spectral matrices (Pham, 2002). This algorithm exploits source coloration, a marked characteristic of both EEG and iEEG tracings. With EEG and iEEG recorded simultaneously, we computed all pair-wise temporal correlations between iEEG poles 1-8 and the 18 extracted independent components of EEG. The correlations were computed over all 184 seconds (23552 samples). Exactly the same method was applied to recordings of simultaneous scalp EEG and poles 9-16 of the iEEG (180 seconds, or 23040 samples).

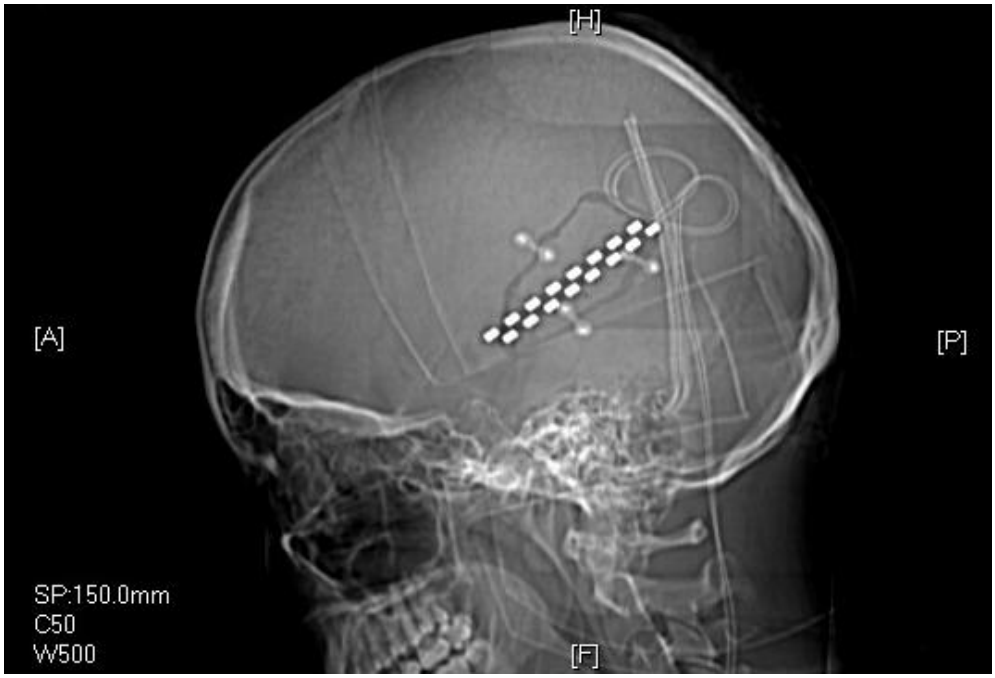

Figure 1. *CT scan with intra-cranial electrode consisting of two rows of 8 poles (lower row: poles 1-8 anterior to posterior; upper row: poles 9-16 anterior to posterior) on left auditory cortex.*

3. Results

As per definition of ICA, the 18 independent components are all pair-wise uncorrelated (top-left blocks of Fig. 2). On the other hand, the 8 iEEG time series of the lower and upper electrode row are strongly correlated (bottom-right blocks) inversely with distance, as expected by their proximity according to EEG volume conduction theory (Nunez and Srinivasan, 2006). Looking at the tracings of the lower row of the iEEG (poles 1-8) a strong correlation is found for two of the 18 extracted independent components (ICs) (Fig. 2, left, top-right or bottom-left block). The correlated components are IC 3 and IC 4. The maximum current density value of IC 3 is localized on the left inferior parietal lobe (BA40), and extends to the temporal lobe (see Fig. 3 top). This component correlates well with all poles of the intra-cranial electrode ($.54 < r < .72$), but mainly with pole 3, $r=.8$, pole 2, $r=.77$ and pole 1, $r=.72$. IC 4 on the other hand is localized more superiorly on the left superior parietal lobe (BA7; Fig. 3 bottom). This component correlates less with the poles 1-5 ($.27 < r < .39$), but correlates increasingly

with poles 6-8 (respectively, r=.5, r=.6, r=.67). This is in accordance with the location of the intra-cranial electrode poles going from anterior to posterior.

EEG data recorded simultaneously with the upper row (poles 9-16) of iEEG electrode was strongly contaminated by EMG; one of such contamination is generated by the left jaw and is separated as IC 18 (Fig. 6). Despite the contamination affects the electrode closest to the left temporal source, IC 7 has localisation very similar to IC 3 previously found (Fig.4) and is highly correlated with the iEEG recordings (max r=0.64). The other source correlating well with iEEG is occipital (IC 1, max r=0.54). Furthermore (data not shown) all intra-cranial electrode poles correlate highly with T3 (.63 <r<.77) and T5 (.59 <r<.8) scalp electrodes, but far less with other scalp electrodes.

Figure 2. *Correlation matrix 18 EEG ICs and of Left: 8 lower- poles of iEEG, right: 8 upper- poles of iEEG*

Interestingly, the ICA algorithm detects two sources explaining the iEEG recordings. Inspecting the time series of the lower row iEEG and associated EEG IC 3-4, a strong correspondence between iEEG and EEG source signals is seen (see Fig. 6). As compared to IC 4, IC 3 has more low-frequency energy (2-7Hz); however, the spectral profile is very similar for both sources (Fig. 5). Similar findings were obtained on the upper electrodes (Fig. 6).

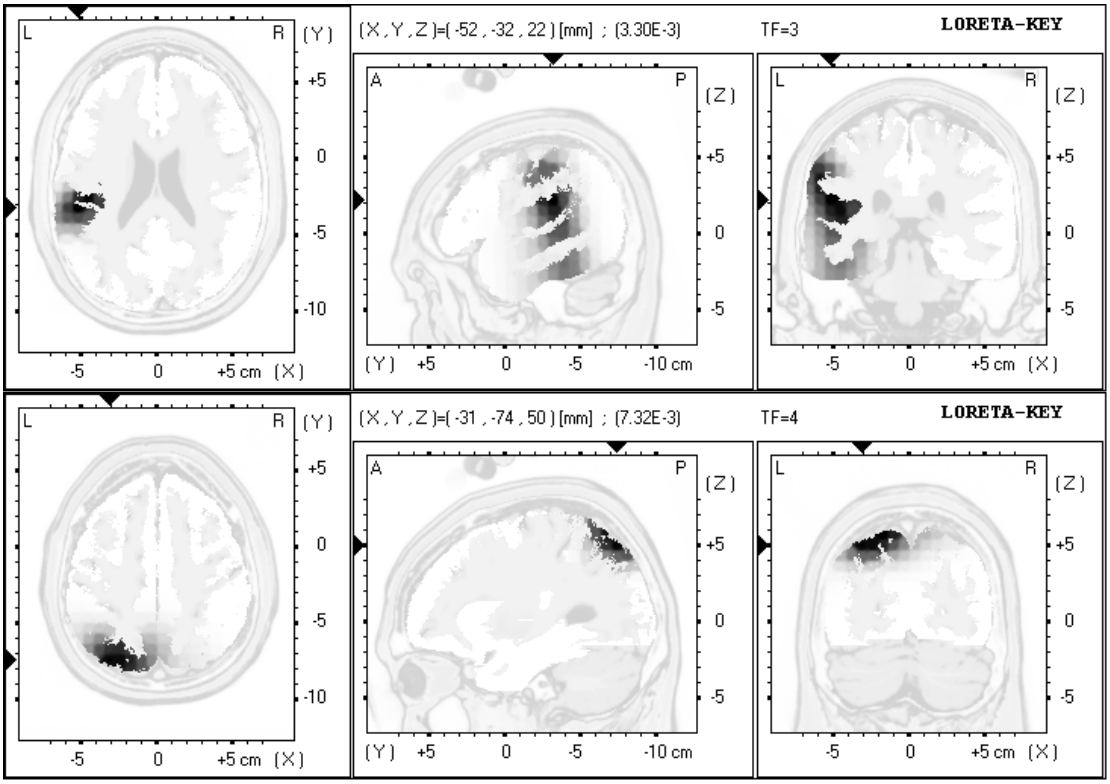

Figure 3. *sLORETA localisation of IC 3 (top) and IC 4 (bottom) of theEEG recorded simultaneously with the lower row. From left to right is the axial, sagittal and coronal view through the maximum.*

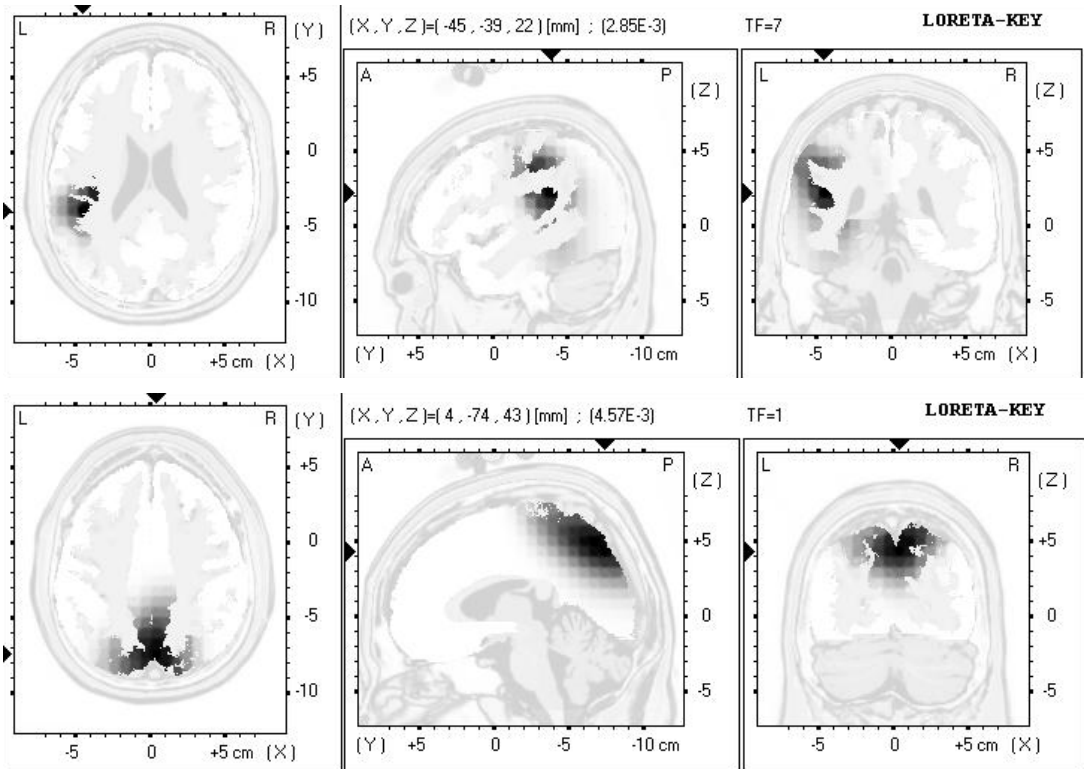

Figure 4. *sLORETA localisation of IC 7 (top) and IC 1 (bottom) of theEEG recorded simultaneously with the upper row. From left to right is the axial, sagittal and coronal view through the maximum.*

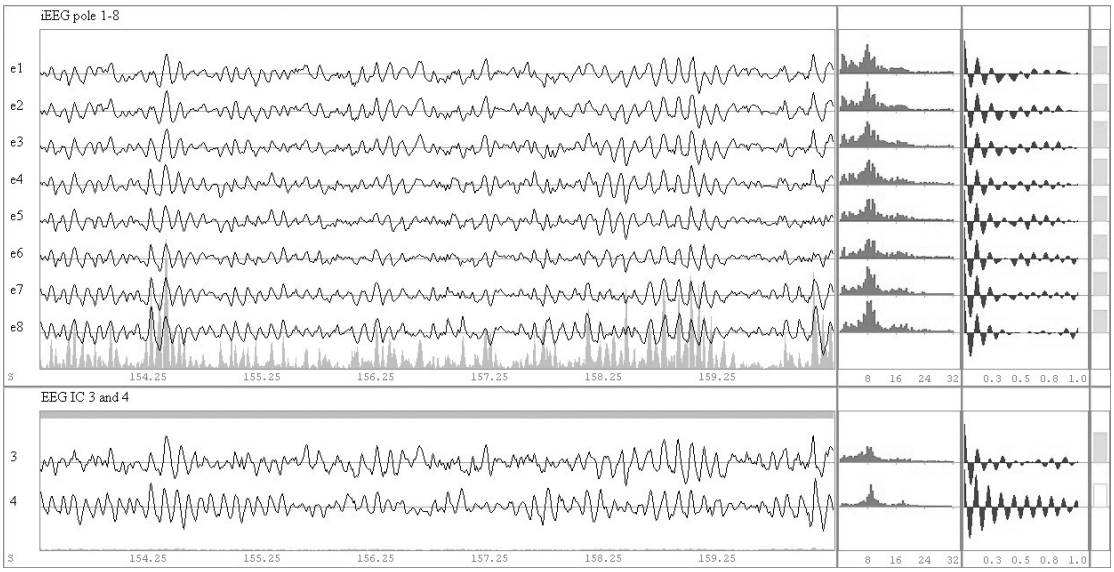

Figure 5. *Seven seconds of time series of the 8 lower intra-cranial poles 1-8 (top), and independent components 3 and 4 (bottom), along with the Fourier power spectra (1-32 Hz), autocorrelation (lag 0 to 1 sec) and Hurst exponent.*

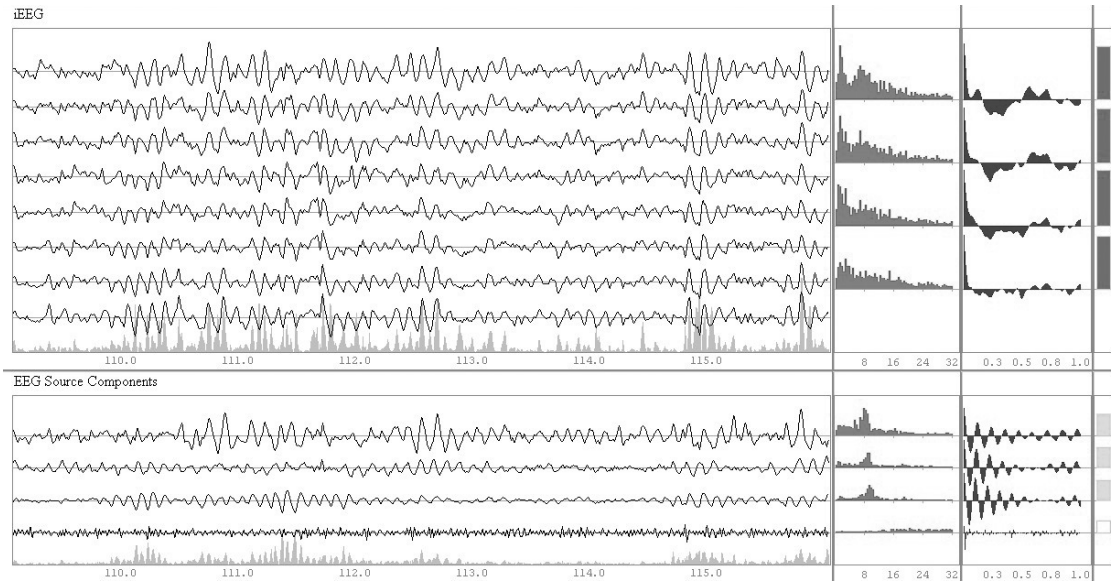

Figure 6. *Seven seconds of time series of the 8 upper intra-cranial poles 9-16 (top), and independent components 7, 2, 1, 18 (bottom), along with the Fourier power spectra (1-32 Hz), autocorrelation (lag 0 to 1 sec) and Hurst exponent.*

4. Discussion

EEG is a commonly used method to measure brain activity. However due to physical properties of the head (especially the skull) the signal is smeared out. Intra-cranial electrode recordings (iEEG) give a unique way to measure brain activity directly at the site of the electrode, bypassing skin, muscle and skull resistance. Comparing extra-dural intra-cranial recordings to scalp EEG in one patient, validation of the independent components (ICs) at the site of the electrode is presented. In both recordings (scalp EEG and lower row iEEG, and scalp EEG and upper row iEEG) respectively two and three of the eighteen ICs highly correlate with the iEEG recording. The ICs on the temporal source of both scalp EEGs overlap quiet well. It seems that beside the main auditory cortex source other brain sources were picked up by the iEEG. The lower electrode row correlates strongly with a left parietal source, possibly due to proximity of the source. In addition, the upper electrode correlates strongly with an occipital alpha source, possibly caused by the high power of this source. As the intra-cranial electrode is placed onto the dura, possible smearing can still be expected through cerebrospinal fluid and/or dura. Other factors like electrode positioning or head shape could also be of influence since we have been using a standard head model. The increasing correlation of the iEEG poles, with higher correlation for the poles closer to this component, nevertheless suggest the location of a component posterior to the electrode is strong enough to be picked up by the iEEG due to volume conduction. The EMG contamination of the scalp EEG recording is clearly seen in a second left temporal component in the upper electrode, with a typical Fourier power spectra created by muscle tension. The fact that this component correlates with iEEG recordings suggest that the electric field created by the muscle has reached the underlying iEEG electrode trough the skull.

Considering this patient was implanted to relieve her from tinnitus, the IC on the temporal lobe could potentially represent the tinnitus pathology. According to our data the EEG ICA source localized in the auditory cortex may be a better representation of the pathological source as compared to iEEG recording; in fact, iEEG recordings seems a mixture of the target and other brain sources. If confirmed by further recordings in other patients, the representation of tinnitus by ICA of scalp EEG could serve as a neural correlate of tinnitus similarly to what has been suggested for contra-lateral auditory cortex gamma band activity (Llinas et al., 1999, Weisz et al., 2007). These findings suggest that the ICs are a good estimation of the sources generated in the regions underlying the iEEG electrodes. Furthermore, the very low correlation between the iEEG time series and the remaining ICs suggests that the EEG can be filtered, excluding the influence of the other ICs, leaving only the scalp projection of these sources. Further investigations on more patients will be performed to confirm these findings.

References

Pascual-Marqui RD, Standardized low-resolution brain electromagnetic tomography (sLORETA): technical details. Methods Find. Exp. Clin. Pharmacol, 24: 5–12 (Suppl D), 2002.

Cichocki A, Amari S. Adaptive Blind Signal and Image Processing Learning Algorithms and Applications John Wiley & Sons, New-York, 2002.

De Ridder D, De Mulder G, Menovsky T, Sunnaert S, Kovacs S. Electrical stimulation of auditory and somatosensory cortices for treatment of tinnitus and pain. *Prog Brain Res*, 166:377-88, 2007.

Congedo M. Subspace Projection Filters for Real-Time Brain Electromagnetic Imaging, IEEE Transactions on Biomedical Engineering, 53(8): 1624-34., 2006.

Nunez PL, Srinivasan R. Electric Field of the Brain, 2nd ed., New York: Oxford Univ. Press, 2006.

Pham D-T. Exploiting source non stationary and coloration in blind source separation. *Digital Signal Processing* 1: 151-154, 2002.

Llinas RR, Ribary U, Jeanmonod D, Kronberg E, and Mitra PP. Thalamocortical dysrhythmia: A neurological and neuropsychiatric syndrome characterized by magnetoencephalography. *PNAS*. 96: 15222-15227, 1999.

Weisz N, Müller S, Schlee W, Dohrmann K, Hartmann T and Elbert T. The neural code of auditory phantom perception. *The journal of neuroscience* 27(6): 1479-1484, 2007.